Transactions on Computer Science and Intelligent Systems Research
ISSN: 2960-1800, eISSN: 2960-2238 | Volume 12
ESAC 2026

MATLAB-Simulation-Based Analysis of Free RLC Oscillations

Jingbin Xue *, Yuyang Qi, Dechao Lv
School of physics, Hangzhou Normal University, Hangzhou, China, 311121
* Corresponding Author Email: 2025112030019@stu.hznu.edu.cn

Abstract. Targeting the LC oscillation commonly taught in high school, this study models a resistive RLC circuit using university-level circuit theory and ODE tools. We compare time responses and energy dissipation under under-, critical-, and over-damping, and visualize charge, current, and total energy via MATLAB. The work offers a quantitative, reproducible framework to bridge high-school and university instruction and to tune experimental parameters, while clarifying often-confused issues (e.g., trends of the Q factor). Innovations: (1) a classroom-oriented simulation pipeline with ready-to-use plots; (2) a unified, dimensionless and energy-based formulation covering all three damping regimes; (3) practical guidance on selecting R, L, and C to achieve target behaviors.

Keywords: LC oscillation; RLC model; damping characteristics.

1. Introduction

LC oscillation circuit, with the energy exchange between inductance and capacitance as its core, is an important content that connects high schools, universities, and even electronic information engineering. Its mathematical form is isomorphic to the harmonic vibration situation in mechanics, and is often reduced to second-order constant coefficient differential equations under linear quantitative assumptions [1-4]. However, in real situations, LC oscillation circuits are often non ideal and inevitably have resistance, resulting in the temporal variation of current, voltage, and energy being divided into three categories: underdamped, critical damped, and over damped; Energy is no longer conserved, and the frequency of the circuit also changes [5]. In recent years, research on primary courses and experimental teaching in universities has further clarified several "textbook impressions": for example, the "counterintuitive" phenomenon of the quality factor of parallel RLC increasing with resistance, and new evidence for time optimization problems such as "which damping first returns to the threshold energy" [6-8]; At the same time, the teaching practice of numerical calculation has also demonstrated the feasible path of using simulation to connect parameters, waveforms, and energy [9-10]. Based on this, this article will take the common LC circuit in high school as the starting point, and systematically analyze the numerical solution and simulation images of resistive LC oscillation circuits, providing new evidence support for the teaching of resistive LC circuits.

2. Analysis of Basic LC Oscillatory Circuit

In high school physics, the common LC oscillation circuit consists of an ideal inductor L and an ideal capacitor C, as shown in Figure 1. In the initial state, if a capacitor is charged and the voltage at both ends is, electrical parameters such as current and voltage will oscillate periodically in the circuit, and energy will transfer periodically between the inductor and capacitor. This process essentially corresponds to an undamped harmonic oscillation, whose dynamic equation can be determined by Kirchhoff's law.

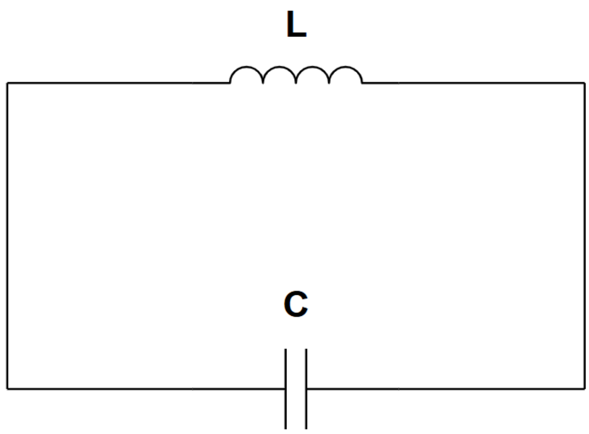

Figure 1. Basic LC oscillation circuit schematic diagram

If the charge on the two plates of a capacitor is $q(t)$ (which should be a function of time with periodic oscillations in the circuit), then the current is $i(t) = \frac{dq}{dt}$. According to Kirchhoff's voltage law:

$$\frac{q}{C} + L\frac{d^2q}{dt^2} = 0 \tag{1}$$

(1) The equation is a second-order homogeneous linear differential equation, and after organizing it, we obtain

$$\frac{d^2q}{dt^2} + \frac{1}{LC}q = 0 \tag{2}$$

Observing equation (2), its equation form is completely consistent with the motion equation of a harmonic oscillator, where the angular frequency is $\omega = \frac{1}{\sqrt{LC}}$.

Therefore, the oscillation period of the circuit is $T = 2\pi\sqrt{LC}$, which is determined only by the size of the inductance and capacitance, and is independent of the initial charge carried by the capacitance. Equation (2) yields the variation of charge over time:

$$q(t) = Q\cos(\omega t + \varphi) \tag{3}$$

It can be seen that Q and φ in equation (3) are determined by the initial conditions. We set the initial charge of the capacitor to Q_0 and the initial current in the circuit to zero, and we can obtain:

$$q(t) = Q_0\cos(\omega t) \tag{4}$$

$$i(t) = -Q_0\omega\sin(\omega t) \tag{5}$$

From this, it can be seen that charge and current have a trigonometric relationship with time, and there is a phase difference of $\frac{\pi}{2}$ between the two, that is, the two parameters of current and charge reach their extremum when they are zero to each other. In fact, this reflects the mutual conversion between electric field energy and magnetic field energy. We use energy analysis of capacitors and inductors to more intuitively reveal the physical essence of oscillation processes. Substituting equations (4) and (5) into the energy expression for capacitors and inductors, we have

$$W_C(t) = \frac{Q_0^2}{2C}\cos^2(\omega t) \tag{6}$$

$$W_L(t) = \frac{Q_0^2}{2C}\cos^2(\omega t) \quad (7)$$

The sum of the two is exactly $\frac{Q_0^2}{2C}$, constant and unchanging. This indicates that an ideal LC oscillation circuit does not generate energy loss during operation, and energy is only continuously converted between capacitors and inductors: when the capacitor is fully charged, all energy is stored in the form of an electric field; As the charge is released, the current gradually increases, and the magnetic field energy in the inductor accumulates accordingly; When the current reaches its maximum value, energy is completely converted into magnetic field energy. Afterwards, the process proceeds in reverse, and the energy returns to the capacitor, forming periodic oscillations. The author used MATLAB simulation to plot the changes in current charge (Figure 2) and energy (Figure 3) over time.

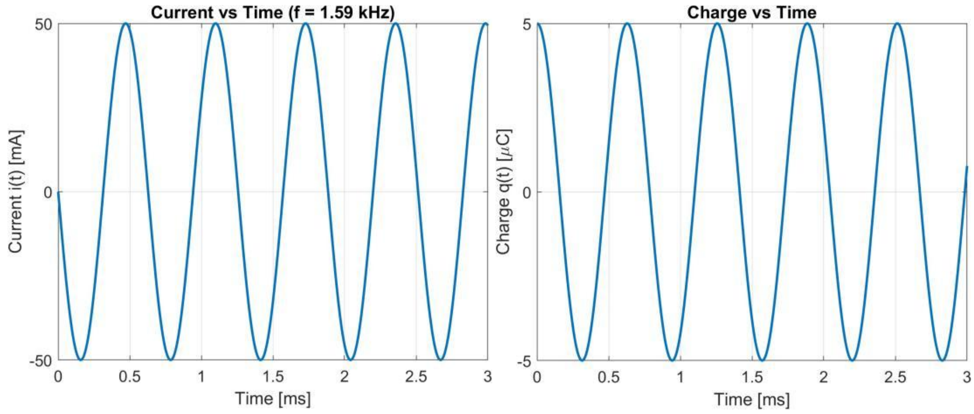

(a) Current Time Variation Diagram (b) Charge Time Variation Diagram

Figure 2. Schematic diagram of current and charge changes over time

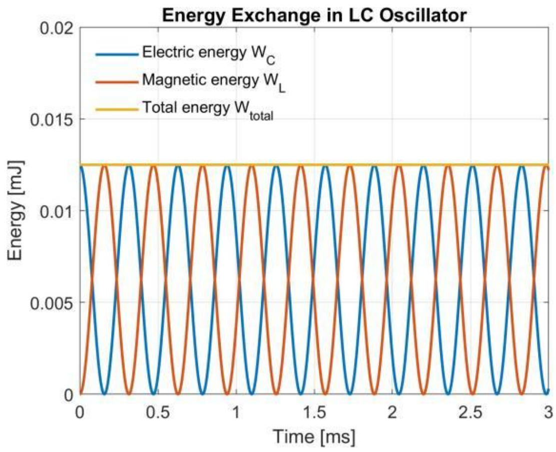

Figure 3. Schematic diagram of energy variation over time

In summary, the dynamic essence of basic LC oscillation circuits lies in the fact that the charge satisfies the harmonic oscillation equation, and its period is only determined by the component parameters L and C. Capacitors and inductors serve as "storage tanks" for energy, achieving lossless exchange between electric field energy and magnetic field energy. This process not only reveals the universal laws of electromagnetic oscillation, but also lays a theoretical foundation for further discussions on complex situations involving damping and external power sources.

3. LC oscillation circuit with resistance

3.1. Modeling and parameter characterization of resistive RLC free oscillation

A resistive LC oscillator circuit refers to a circuit component that includes capacitors, inductors, and resistors, as shown in Figure 4.

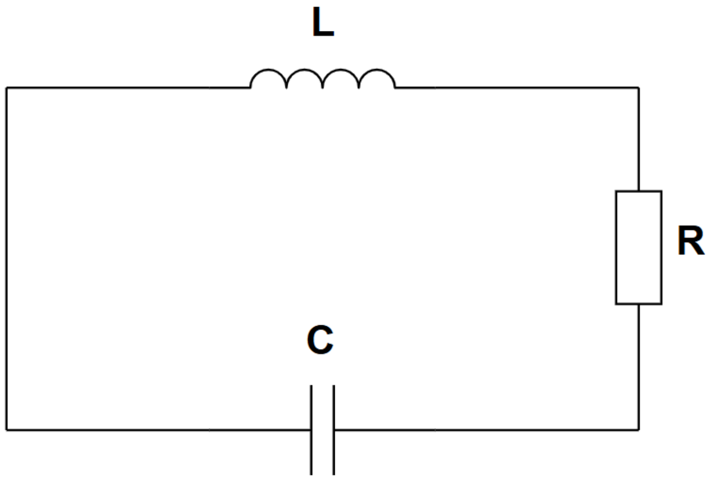

Figure 4. Schematic diagram of LC oscillation circuit with resistance

According to Kirchhoff's law, it is known that:

$$L\frac{d^2q}{dt^2} + R\frac{dq}{dt} + \frac{q}{C} = 0 \tag{8}$$

Equation (8) is a second-order linear homogeneous differential equation with constant coefficients, whose structure is completely isomorphic to the damping oscillator in mechanics. For the convenience of physical interpretation and parameterization, two key parameters are introduced: unobstructed natural angular frequency WW and damping coefficient AA, and further normalized by dimensionless time TT. Equation (8) can be expressed as

$$\frac{d^2q}{d\tau^2} + 2\zeta\frac{dq}{dt} + q = 0 \tag{9}$$

Among them, $\zeta = \frac{R}{2}\sqrt{\frac{C}{L}}$ represents the damping ratio, and the magnitude of the damping ratio is an important basis for classifying the three types of damping behaviors. For the case of underdamped $\zeta < 1$, the circuit oscillates and decays; For the critical damping scenario $\zeta = 1$, the circuit oscillates back to zero the fastest; For the case of over damping $\zeta > 1$, the circuit exhibits exponential decay. The most common situation in high school is under damping, where the amplitude decays exponentially and the frequency is slightly lower than ω_0.

To connect the above analysis with the concept of energy, this article defines the instantaneous total energy of capacitors and inductors as:

$$W(t) = \frac{q^2}{2C} + \frac{1}{2}Li^2 \tag{10}$$

From equation (10) and Kirchhoff equation, we can obtain:

$$\frac{dW}{dt} = U_C i + U_L i = -i^2 R < 0 \tag{11}$$

Equation (11) reveals the essence of damping: in an ideal LC, the electric field energy and magnetic field energy alternate without loss, but with the introduction of resistance, the energy will be converted into Joule heat at an instantaneous power of, causing the average energy to continuously decay over time. On the other hand, according to equation (9), the energy decay constant is known to be $\tau_E = \frac{1}{2\alpha} = \frac{L}{R}$.

From this, a relatively clear tuning guideline can be summarized: under the given inductance and capacitance conditions, increasing the resistance will accelerate energy dissipation, enhance damping, and reduce the actual oscillation frequency; On the contrary, reducing resistance or increasing capacitance is beneficial for maintaining oscillation, which is often introduced in engineering as a quality factor $Q = \frac{w_0 L}{R}$ to represent the durability of vibration.

3.2. Analytical solutions and numerical simulations for three damping scenarios

3.2.1. Underdamped situation.

If the eigenvalues corresponding to the characteristic equation (9) of $\zeta < 1$ are virtual roots, this paper still uses the initial charge quantity of Q_0 and the initial current of zero. According to the solution of the second-order linear homogeneous differential equation with constant coefficients, we obtain:

$$q(t) = Q_0 e^{-\alpha t}(\cos \omega_d t + \frac{\alpha}{\omega_d} \sin \omega_d t) \tag{12}$$

$$i(t) = -Q_0 \frac{\omega_0^2}{\omega_d} e^{-\alpha t} \sin \omega_d t \tag{13}$$

This article uses MATLAB to numerically simulate the current, voltage, and energy conditions during the process, and the results obtained are shown in Figures 5 and 6.

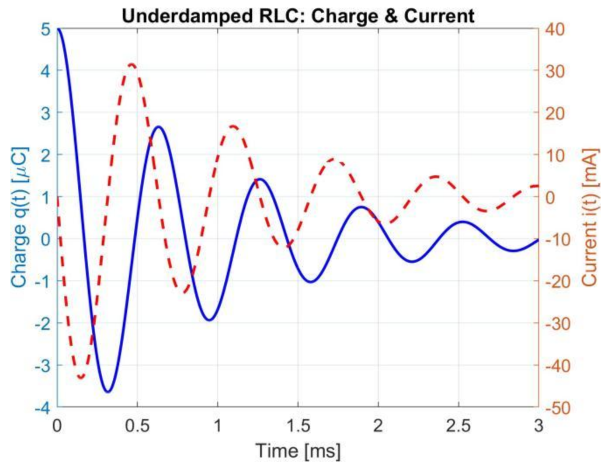

Figure 5. Schematic diagram of current and voltage changes over time under underdamped conditions

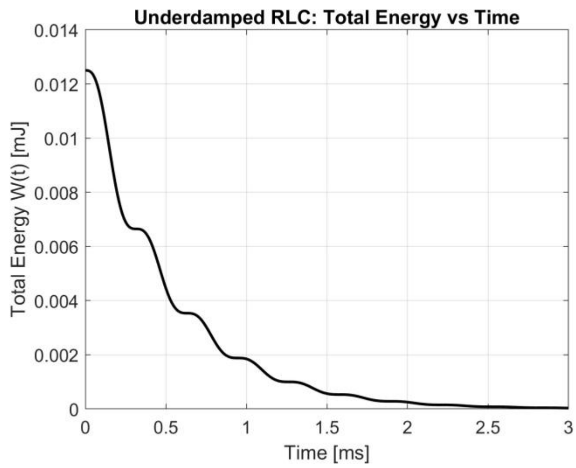

Figure 6. Schematic diagram of total energy variation over time under underdamped conditions

In Figure 5, both traces show ringing with progressively smaller peaks and troughs. The zero crossings of the two curves do not align with their extrema, revealing a persistent phase offset. The earliest cycles are the strongest; each subsequent cycle is weaker, and the overall pace appears slightly stretched compared with an ideal lossless picture. Figure 6 presents a strictly decreasing total-energy curve. Local bumps are visible, yet each bump is lower than the previous one, giving a staircase-like decline. Taken together, the two plots display a "strong-to-weak, oscillate-while-fading" pattern and a gradual, smooth return toward the baseline.

3.2.2. Critical Damping Scenario.

If $\zeta < 1$, the double eigenvalues corresponding to the characteristic equation in equation (9) coincide, according to equation (9), we can solve for:

$$q(t) = Q_0(1 + \alpha t)e^{-\alpha t} \tag{14}$$

$$i(t) = -Q_0\, \alpha^2\, t\, e^{-\alpha t} \tag{15}$$

Numerical simulations were conducted on it, and the results are shown in Figures 7 and 8.

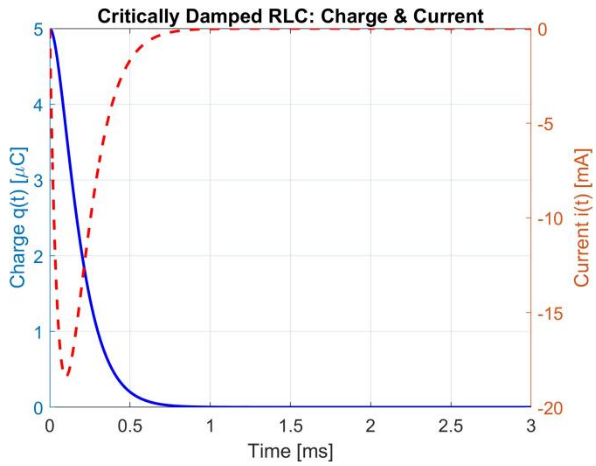

Figure 7. Schematic diagram of current and voltage variation with time under critical damping conditions

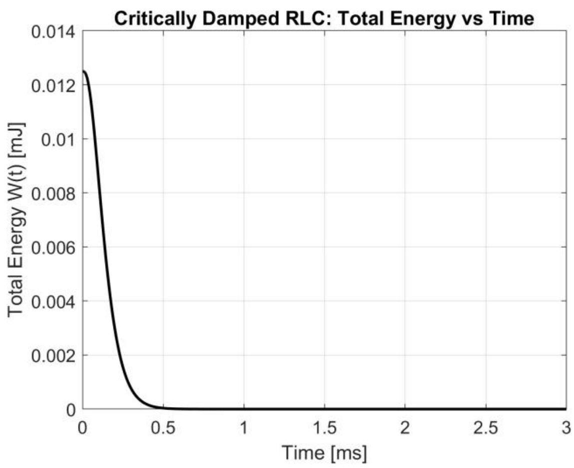

Figure 8. Schematic diagram of total energy variation over time under critical damping conditions

In Figure 7, repeated oscillations are absent. The charge trace moves toward the baseline quickly and smoothly, while the current shows a single pronounced pulse and then collapses, with no overshoot or ringing. Figure 8 shows the total energy dropping most steeply at the beginning and then approaching a very low level in short order; the curve is nearly perfectly monotonic and smooth. Read together, the plots highlight a non-oscillatory, rapidly settling behavior with minimal residual fluctuation near the baseline

3.2.3. Over damping situation.

If $\zeta < 1$, the characteristic equation corresponding to equation (9) has two different real roots. Note:

$$s_{1,2} = -\alpha \pm \sqrt{\alpha^2 - \omega_0^2}, (s_1 < s_2 < 0) \tag{16}$$

According to the form of the solution of the second-order linear homogeneous differential equation with coefficients, obtain

$$q(t) = Q_0 \cdot \frac{s_1 e^{s_2 t} - s_2 e^{s_1 t}}{s_1 - s_2} \tag{17}$$

$$i(t) = Q_0 \cdot \frac{s_1 s_2}{s_1 - s_2}(e^{s_2 t} - e^{s_1 t}) \tag{18}$$

Numerical simulations were conducted on it, and the results are shown in Figures 9 and 10.

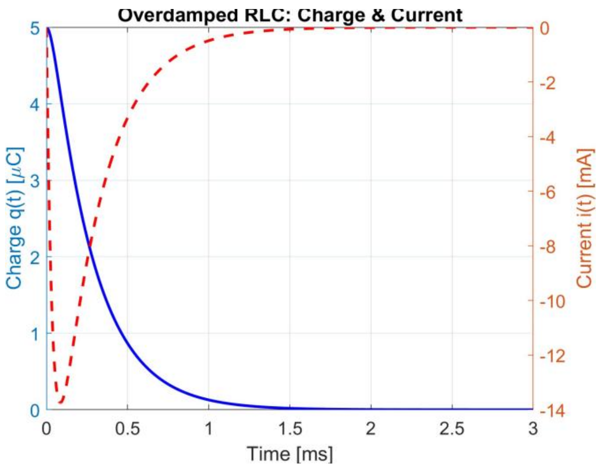

Figure 9. Schematic diagram of the variation of current and voltage over time in the case of over damping

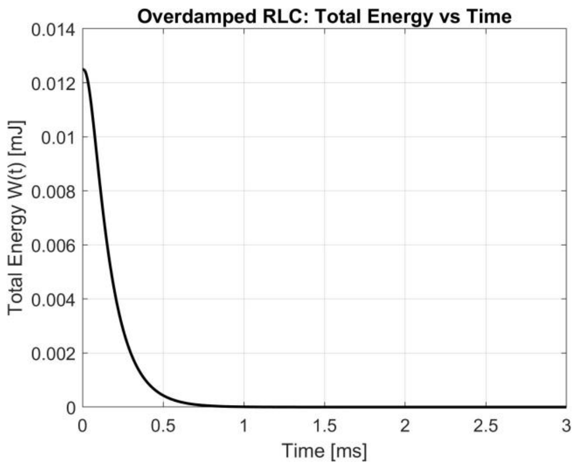

Figure 10. Schematic diagram of total energy variation over time in the case of over damping

Figure 9 exhibits a non-oscillatory response with the slowest return to the baseline. Both charge and current decay quickly at first and then enter a pronounced long tail, staying close to the baseline for an extended period without clear overshoot. Zero-crossing events are rare. In Figure 10, the total-energy curve is also monotonic but clearly two-stage: a rapid initial drop followed by a prolonged, gentle decline that hovers near a low level. Together, the plots reveal a pattern of no oscillation, the longest settling time, and a prominent long-tail behavior.

4. Conclusion

This work provides a unified comparison of the time evolution of charge, current, and total energy under underdamped, critically damped, and overdamped conditions, with side-by-side plots that make the contrasts explicit. Building on these results, we establish a compact workflow—simulation, parameter tuning, plot interpretation, and experimental verification—that uses standard components, runs quickly, and yields reproducible visuals with good transferability across instruments. Looking forward, we will incorporate non-ideal effects and uncertainty, provide structured error analysis, and complement the free response with driven tests to document steady-state and sweep behavior. We will also develop an interactive interface with automatic parameter identification to align simulated traces with measured data, and curate an open repository of reference plots and datasets. Together, these extensions aim to enhance precision, transparency, and reusability while keeping the approach lightweight and easy to reproduce.

References

[1] Faleski M C. Transient behavior of the driven RLC circuit [J]. American Journal of Physics, 2006, 74 (5): 429–437.

[2] Bissell J J. On the ubiquity of classical harmonic oscillators and a universal equation for the natural frequency of a perturbed system [J]. American Journal of Physics, 2021, 89 (12): 1094–1102.

[3] Westermann N, Staacks S, Heinke H, Möhrke P. Measuring the magnetic field of a low-frequency LC-circuit with phyphox [J]. Physics Education, 2022, 57 (6): 065024.

[4] Agarwal A., Lang J. Foundations of Analog and Digital Electronic Circuits [M]. Morgan Kaufmann/Elsevier, 2005.

[5] OpenStax. University Physics Volume 2: 14.5 Oscillations in an LC Circuit [EB/OL]. 2016-10-06 [2025-09-15].

[6] Paulson J. G., Ray M. W. "Exploration of the Q factor for a parallel RLC circuit" [J]. American Journal of Physics, 2022, 90 (12): 903–907.

[7] Lelas K., Poljak N., Jukić D. "Damped harmonic oscillator revisited: The fastest route to equilibrium" [J]. American Journal of Physics, 2023, 91 (10): 767–772.

[8] Kowalski F. V., Swantek J. L., D'Esposito T., Brannum J. "Voltage decay in an RLC circuit is not what is taught: An advanced laboratory exercise" [J]. American Journal of Physics, 2024, 92 (3):186–188.

[9] Alizadeh S., et al. "Analyzing transient response of the parallel RCL circuit by Caputo–Fabrizio derivative" [J]. Advances in Continuous and Discrete Models, 2020, 2020: 357.

[10] Ahmed F, Iqbal M, Tariq I, Talat M. Virtual learning via spreadsheets: Real-time simulation of an RC circuit [J]. American Journal of Physics, 2024, 92 (5): 328.